

## Accelerator Measurement of the Energy Spectra of Neutrons Emitted in the Interaction of 3-GeV Protons with Several Elements

W. J. Nalesnik, T. J. Devlin\*, M. Merker, and B. S. P. Shen

Astrophysics Laboratory and Princeton-Pennsylvania Accelerator,  
University of Pennsylvania, Philadelphia, Pennsylvania

**Abstract** - The shapes of the energy spectra of neutrons between 20 and 400 MeV emitted at  $20^\circ$ ,  $34^\circ$ , and  $90^\circ$  in the bombardment of C ( $1.8 \text{ g cm}^{-2}$ ), Al ( $1.7 \text{ g cm}^{-2}$ ), Co ( $4.4 \text{ g cm}^{-2}$ ), and Pt ( $81.5 \text{ g cm}^{-2}$ ) targets by 3-GeV protons have been measured by time-of-flight techniques.

In the study of the mechanism of spallation reactions (ref. 1), in certain aspects of astrophysics and geophysics (ref. 2), and in high-energy shielding and dosimetry (ref. 3), it is often important to know the energy spectrum of neutrons emitted in spallation reactions induced by high-energy protons. This paper gives a preliminary report of our measurements of such spectra at the Princeton-Pennsylvania Accelerator. We present here neutron spectra from 20 to 400 MeV at  $20^\circ$ ,  $34^\circ$ , and  $90^\circ$  for 3-GeV protons incident on cylindrical targets of carbon ( $1.8 \text{ g cm}^{-2}$  diameter), aluminum ( $1.7 \text{ g cm}^{-2}$  diameter), cobalt ( $4.4 \text{ g cm}^{-2}$  diameter), and on a  $0.64 \text{ cm} \times 0.64 \text{ cm} \times 81.5 \text{ g cm}^{-2}$  thick platinum target.

Figure 1 shows the experimental arrangement. The target being bombarded is located in the internal circulating beam of the accelerator. Collimated neutral beams emerge from the target at  $20^\circ$ ,  $34^\circ$ , and  $90^\circ$  degrees with respect to the direction of the internal beam. Charged particles are removed from the neutral beams by sweeping magnets. We determine neutron energy by measuring the time elapsed between the production of the neutron and its subsequent detection by a plastic scintillator placed in the beam line at a known distance from the target. The target is struck every 269 nanoseconds by a proton bunch approximately one nanosecond in width. The proton beam intensity in this operating mode is on the order of  $5 \times 10^{10}$  protons/second. The length of

the flight path, viz. the distance between the target and the neutron detector, is limited by the accelerator shielding; this determines the lowest energies that can be measured by time of flight. The flight paths are thus 22, 37, and 44 feet at  $90^\circ$ ,  $34^\circ$ , and  $20^\circ$  degrees, respectively. Since we are currently extending our results to lower energies by other techniques, only results for neutron energies greater than 20 MeV are presented here.

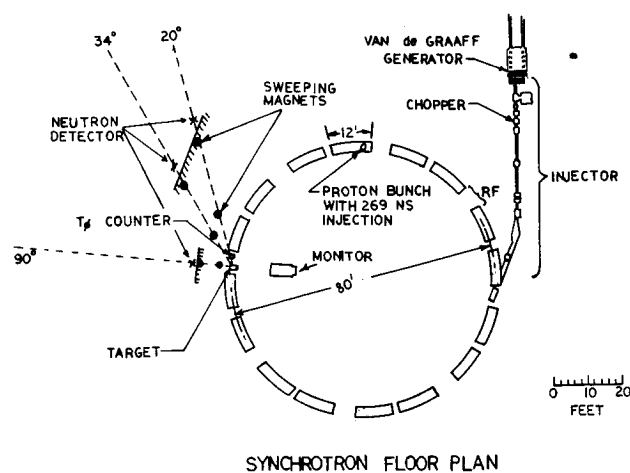


Figure 1. Experimental arrangement at the Princeton-Pennsylvania Accelerator, showing beam lines and detector locations.

\* Department of Physics, Rutgers University, New Brunswick, New Jersey; on leave at CERN, Geneva, Switzerland.

The time at which a neutron leaves the target is determined by the Cerenkov detector T $\emptyset$  located about 2 feet from the target. The neutron detector consists of a 1 inch x 2 inch x 2 inch block of Pilot M scintillator joined to an Amperex 56 AVP photomultiplier by a lucite light pipe. This same detector is used in all three beam lines, with beam particles incident on the 2 inch x 2 inch face. The efficiency of the detector was calculated using the well-known UCRL computer code of R. J. Kurz (ref. 4) modified by Michael Hauser (ref. 5) of Princeton University. This program yields fairly good agreement with experimentally determined efficiencies up to about 150 MeV. The neutron-detector efficiency is given in Figure 2 for thresholds of 1 MeV and 2 MeV electron energy for a detector resolution of 10 %. The 1 MeV threshold was employed for the 90 degree cases, and the 2 MeV threshold for the 20 and 34 degree cases.

Each time a particle is detected, the time delay between the most recent T $\emptyset$  pulse and the neutron detector particle signal is measured by a time-to-amplitude converter (ref. 6). Its output, together with the neutron detector pulse height, is fed to a PDP-9 computer which records these data for each event. The computer also provides on-line display of the time-of-flight spectrum and the pulse-height distributions as a function of time-of-flight. Scalers also monitor the integral neutron detector events as well as other information for the determination of relative beam intensities.

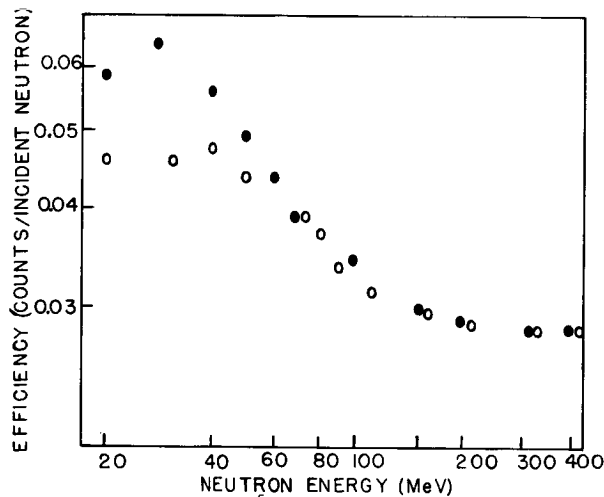


Figure 2. Neutron-detection efficiency as a function of neutron energy, calculated using the Kurz efficiency program. Filled circles are for a threshold of 1 MeV; open circles are for a threshold of 2 MeV.

Figure 3 shows a typical time-of-flight spectrum as displayed by the on-line computer. The peak on the extreme right is due to prompt gamma rays (neutral pion decays, etc.) from the target; all of these gammas have the same flight time. The gamma peak is used as the zero-point for the time determination. The width of the gamma peak at half maximum provides a measure of the time resolution of the system, which is about 2 nanoseconds.

The system is calibrated using the prompt gamma rays as follows. The accelerator is operated in the full injection mode in which there are eight circulating proton bunches per cycle. Thus, the target is struck every 33.65 nanoseconds by a proton bunch, resulting in eight spectra displaced and overlaid in the space occupied by the single spectrum produced by the 269 nanosecond injection. Knowing the distance between each of the eight gamma peaks both in real time and in time-to-amplitude converter channels enables the system to be calibrated to an accuracy of about 2%.

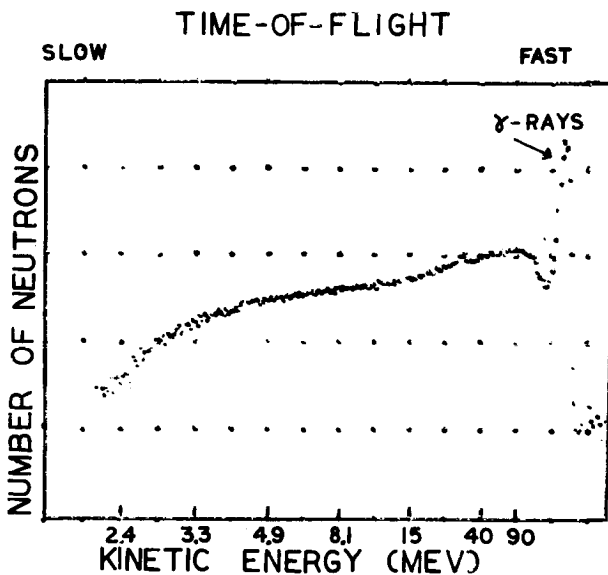


Figure 3. Typical time-of-flight spectrum as displayed by the on-line computer.

Figures 4, 5, and 6 give the relative energy spectra obtained at 20, 34, and 90 degrees, respectively. The histograms are obtained by converting the recorded flight times into energies and collecting them into bins of equal width in log E. The total count in each bin has been divided by the bin width in MeV and the detector efficiency. The error bars represent counting statistical errors only. The effects of activation gammas in the nearby walls have recently been studied and

preliminarily indicate a contribution similar to counting statistics. Contamination of the neutral beams by charged particles has been checked with an anticoincidence scintillator shield. The present results indicate little or no charged particle contamination up to 400 MeV. Overall normalization of the neutron spectra with respect to the number of incident protons has not yet been determined at this writing.

Table 1 gives the approximate inverse-power-law exponents of the spectra shown in Figures 4, 5, and 6 for the energy intervals 20-40 MeV, 40-100 MeV, and 100-400 MeV. It can be seen that, in every case, the spectrum from 40-100 MeV is much less steep than that for either 20-40 MeV or 100-400 MeV. This effect results largely from the shape of the Kurz efficiency curve shown in Figure 3. Table 1 also shows that, in a given energy interval, the spectrum generally tends to steepen with increasing emission angle and, to a lesser extent, with increasing target mass number.

In considering Table 1 and Figures 4, 5, and 6, it should be borne in mind that, while the C, Al, and Co targets are "thin", the Pt target is not ( $81.5 \text{ g cm}^{-2}$  thick).

This research was supported in part by NASA and USAEC.

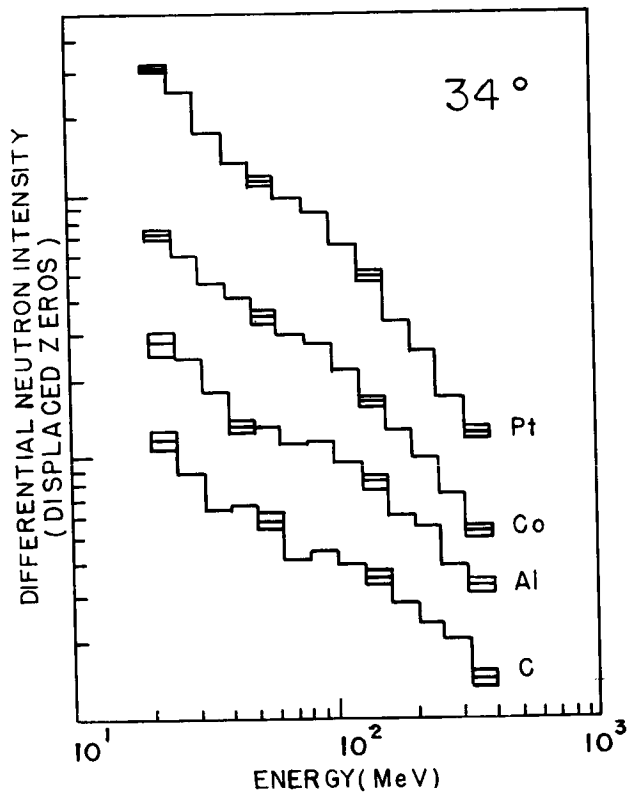


Figure 5. Same as Figure 4, at  $34^\circ$  emission angle.

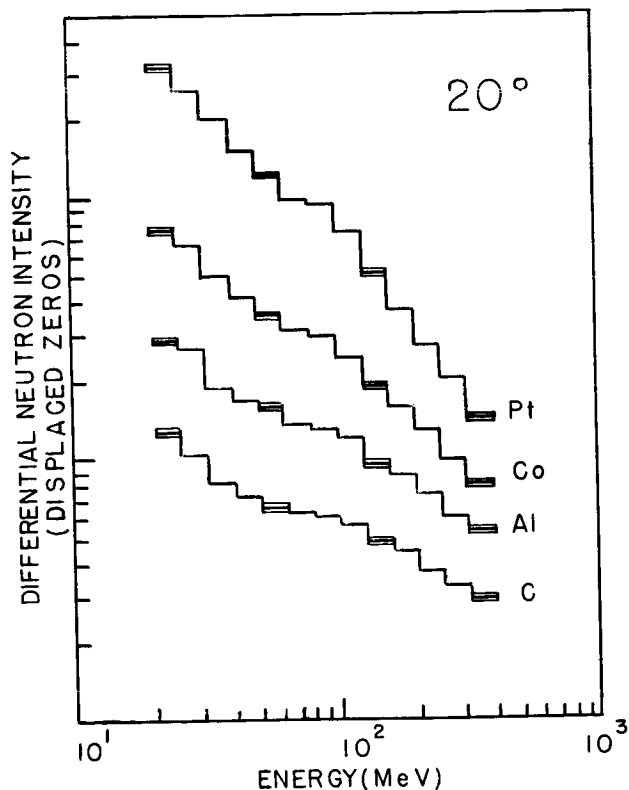


Figure 4. Measured differential neutron spectra for neutrons emitted at  $20^\circ$  from targets bombarded by 3-GeV protons. Representative counting statistical errors are indicated in several energy bins by triple-lined histogram segments.

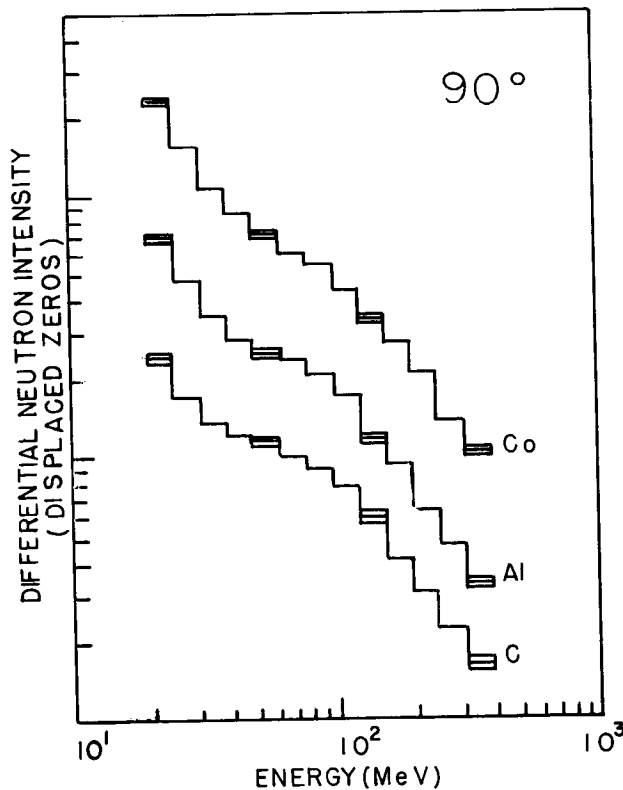


Figure 6. Same as Figure 4, at  $90^\circ$  emission angle.

Table 1. Approximate Inverse Power-Law Exponents of Neutron Spectra

Target	Energy Interval (MeV)	20°	34°	90°
C	20-40	0.8	1.0	1.2
	40-100	0.2	0.5	0.4
	100-400	0.6	1.0	1.3
Al	20-40	0.8	0.9	1.4
	40-100	0.4	0.3	0.4
	100-400	0.7	1.0	1.3
Co	20-40	0.8	0.9	1.4
	40-100	0.5	0.6	0.6
	100-400	1.0	1.2	1.2
Pt	20-40	1.0	1.2	
	40-100	0.6	0.7	
	100-400	1.5	1.4	

#### REFERENCES

1. G. Friedlander, J. W. Kennedy, and J. M. Miller, Nuclear and Radiochemistry (J. Wiley, New York, 1964), p. 316.
2. B. S. P. Shen, ed., High Energy Nuclear Reactions in Astrophysics (W. A. Benjamin, New York, 1967), p. 1.
3. B. S. P. Shen, *Astronautica Acta*, vol. 9, p. 211 (1963).
4. R. J. Kurz, A 709/7090 Fortran II Program to Compute the Neutron-Detection Efficiency of Plastic Scintillator for Neutron Energies from 1 to 300 MeV, UCRL-11339 (1964).
5. M. Hauser, private communication, 1971.
6. P. F. Shepard, T. J. Devlin, R. E. Mischke, and J. Solomon, N - P Charge Exchange Between 600 MeV/c and 2000 MeV/c, Princeton-Pennsylvania Accelerator Report PPAR-10 (1969).